

THE INFLUENCE OF POINT DEFECTS ON THE THERMAL CONDUCTIVITY OF GRAPHENE

S. CHANDRA AND POOJA RANI

Department of Physics, Panjab University, Chandigarh-160014, India

RECEIVED : 22 August, 2016

In this paper we shown that the experimentally observed increase of Young's modulus in single layer graphene with low density of point defects leads to a noticeable enhancement of the thermal conductivity in a wide temperature range.

KEYWORDS : Thermal properties of graphene, Graphene, Elastic moduli.

INTRODUCTION

Recently, the effect of mechanical stiffness augmentation in grapheme by controlled creation of a low density of point vacancy defects through Ar^+ irradiation has been experimentally revealed [1]. It has been found that Young's modulus (E_{2D}) of the graphene membrane increases with increasing irradiation dose and reaches a maximum of 550 Nm^{-1} at 0.2% defect content. For a higher defect content a decreasing E_{2D} has been observed. This effect was attributed to the suppression of the out-of-plane fluctuations by defects.

The atomic simulation shows that this effect is mainly originated from a specific bonds distribution in the surrounded monovacancy defects [2]. Moreover, it has been shown that such unusual mechanical response is the feature of the presence of specifically monovacancies, whereas other types of point defects such as divacancy, 555-777 and Stone-Wales defects lead to the ordinary degradation of the grapheme mechanical stiffness [2]

Notice that this unusual behavior will affect other important properties of defected grapheme. In this paper, we consider a possible impact of mono vacancy defects at a tiny concentration on the phonon thermal conductivity of grapheme. Physically, a growing number of point defects will enhance the phonon scattering thus leading to the reduction in the thermal conductivity. In our case, however the increase of Young's modulus will result in the increased sound velocities, which reduces anharmonic phonon-phonon scattering processes and, thereafter, enhances the thermal conductivity. These opposite effects will compete in a wide temperature range. The aim of our paper is to analyze the influence of point defects on the thermal conductivity of graphene within a phenomenological single-mode relaxation time approach with all important scattering mechanisms taken into account. Notice that this simple consideration is sufficient to capture the effect. The detailed discussion of various theoretical approaches to calculation of the phonon thermal conductivity in graphene and graphene nanoribbons can be found in [3-5].

METHODS

The Methods let us start with the well-known definition of sound velocities for longitudinal (LA) and transverse (TA) phonon branches in the isotropic case [6].

$$vLA = \sqrt{E_2 D / \rho(1 - \sigma^2)}, \quad vTA = \sqrt{E_2 D / 2\rho(1 + \sigma)}, \quad \dots (1)$$

where σ is the Poisson's constant, ρ is the material density and Young's modulus is assumed to be a function of the defect density n_{def} . The inset in fig. 1 shows the fit to the measured E_{2D} as a function of defect concentration given in [1].

Here we use Callaway's theory where three-phonon normal processes are taken into consideration explicitly [7]. Notice that the important role of normal phonon scattering processes in graphite-like materials and graphene has been noted in [8-10]. Thus, we consider four main scattering mechanisms relevant for suspended graphene, sample border (rough boundary), point defects, three-phonon normal and umklapp processes. Within the relaxation time approximation the total mean free path can be written as

$$l_{tot, \lambda}^{-1}(q) = l_0^{-1} + l_{pd, \lambda}^{-1}(q) + l_{N, \lambda}^{-1}(q) + l_{U, \lambda}^{-1}(q), \quad \dots (2)$$

where l_0 , $l_{pd, \lambda}$, $l_{N, \lambda}$ and $l_{U, \lambda}$ come from sample border, point defects, three-phonon normal and umklapp scattering, respectively, for a given phonon banch $\lambda = (LA, TA, ZA)$ with the wave vector q . The mean free path due to normal processes is written as [8,10].

$$l_{N, \lambda}^{-1}(q) = B_{N, \lambda} \omega_{2\lambda}^2(q) T^3, \quad \dots (3)$$

and for umklapp phonon scattering processes we employ a parameterized expression in the form

$$l_{U, \lambda}^{-1}(q) = B_{U, \lambda} T^3 \omega_{\lambda}^2(q) \exp(-\Theta_{\lambda} / 3T), \quad \dots (4)$$

Where $B_{N, \lambda}$ and $B_{U, \lambda}$ are parameters and Θ_{λ} is the Debye temperature. It should be mentioned that in our case $B_{(N, U)\lambda} = \bar{B}_{(N, U)\lambda} / v_{\lambda}$, and the numerical values of the parameters $\bar{B}_{N, \lambda}$ and $\bar{B}_{U, \lambda}$ are taken from [8]. $\bar{B}_{N, \lambda} = 2.12 \times 10^{-25} \text{ sK}^{-3}$, $\bar{B}_{U, \lambda} = 3.18 \times 10^{-25} \text{ sK}^{-3}$ for $\lambda = (LA, TA)$ and $\bar{B}_{N, \lambda} = 1.48 \times 10^{-22} \text{ sK}^{-3}$, $\bar{B}_{U, \lambda} = 2.23 \times 10^{-22} \text{ sK}^{-3}$ for $\lambda = (ZA)$.

The boundary scattering is expressed as

$$l_0^{-1} = \frac{1}{d} \quad \dots (5)$$

With d being the effective length determined from the geometry of the graphene sample [8]. The mean free path due to phonon-point defect scattering is taken to be

$$l_{pd, \lambda}^{-1}(q) = \frac{S_0 \Gamma}{4} \frac{q \omega_{\lambda}^2(q)}{v_{\lambda}^2}, \quad \dots (6)$$

where S_0 is the cross-section area per one atom of the lattice, $\Gamma \approx (n_{def}/2) \times 10^{-15} \text{ cm}^{-2}$ is the mass fluctuation phonon scattering parameter in notice that 1% of vacancies corresponds to $n_{def} = 2 \times 10^{13} \text{ cm}^{-2}$ [10].

Within Callaway's formalism, the diagonal components of the thermal conductivity tensor $\kappa(T)$ can be presented by the sum of the Debye term,

$$\kappa_D(T) = \frac{\hbar^2}{2S_0 \kappa_B T^2} \sum_{\lambda} \int d\omega \omega_{\lambda}^2(q) l_{tot, \lambda}(\omega) v_{\lambda} C_{ph, \lambda}(\omega) N_{\lambda}(\omega), \quad \dots (7)$$

and the normal drift term

$$\kappa_N(T) = \frac{\hbar^2}{2S_0 k_B T^2} \times \sum_{\lambda} \frac{[\int d\omega \omega_{\lambda}^2(q) l_{tot, \lambda}(\omega) l_{N, \lambda}^{-1}(\omega) v_{\lambda}^2 C_{ph, \lambda}(\omega) N_{\lambda}(\omega)]^2}{\int d\omega \omega_{\lambda}^2(q) (1 - l_{tot, \lambda}(\omega) l_{N, \lambda}^{-1}(\omega)) l_{N, \lambda}^{-1}(\omega) v_{\lambda}^3 C_{ph, \lambda}(\omega) N_{\lambda}(\omega)}, \dots \quad (8)$$

where $C_{ph, \lambda}(\omega) = \exp(\hbar\omega_{\lambda}(q)/k_B T) / (\exp(\hbar\omega_{\lambda}(q)/k_B T) - 1)^2$ and k_B is the Boltzmann constant. Summation is performed over phonon polarization branches with the dispersion relations $\omega_{\lambda}(q) = qv_{\lambda}$ for $\lambda = LA, TA$. For an out-of-plane (flexural) acoustic mode we use the dispersion law $\omega_{ZA}(q) = q^2/m$ (m is an effective parameter taken here equal to 320 s/cm, $l_{tot, \lambda}(q, T)$ is the phonon mean free path given by eqs. (2)-(6) from [11]. The explicit form of $N_{\lambda}(\omega)$ is taken from [8] as $N_{\lambda}(\omega) = S_{0\omega\lambda}(q)/2\pi v_{\lambda}^2$ for $\lambda = LA, TA$ branches and $N_{ZA}(\omega) = S_0 m/4\pi$.

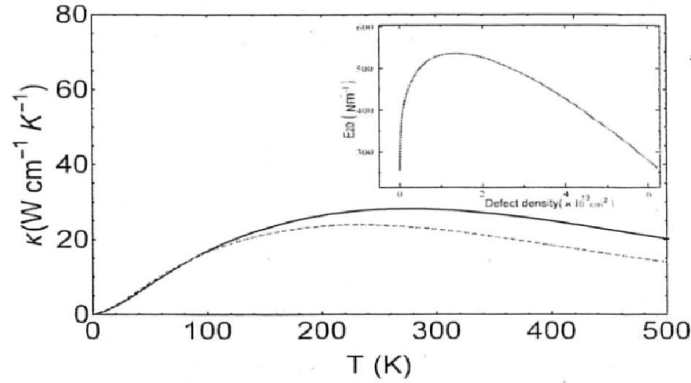


Fig. 1. (Colour online) Thermal conductivity vs. temperature in a 2.9 μm wide ribbon at $n_{def} = 1.5 \times 10^{13} \text{ cm}^{-2}$ in the case of actual (solid line) and constant (dashed line) sound velocities. The insert shows a fit to the experimentally observed Young's modulus as a function of defect concentration.

RESULTS AND DISCUSSION

Fig. 1 shows the calculated $k(T)$ based on eqs. (7) and (8) at the fixed concentration of vacancies $n_{def} = 1.5 \times 10^{13} \text{ cm}^{-2}$ for two cases: (a) the sound velocities do not depend on n_{def} and have fixed values taken from [12]. $v_{LA} = 21.3 \times 10^5 \text{ cm/s}$, $v_{TA} = 13.6 \times 10^5 \text{ cm/s}$ (which corresponds to Young's modulus $E_{2D} \approx 360 \text{ Nm}^{-1}$), and (b) the sound velocities are calculated by eq. (1). For chosen n_{def} one has $E_{2D} \approx 540 \text{ Nm}^{-1}$, so that $v_{LA} = 27.2 \times 10^5 \text{ cm/s}$ and $v_{TA} = 17.2 \times 10^5 \text{ cm/s}$. As seen in fig. 1, in the case of (b) markedly enhanced thermal conductivity takes place in a wide temperature range. The reason is quite clear because larger values of v_{LA} and v_{TA} lead to an increase of $l_{N, \lambda}(q)$ and $l_{U, \lambda}(q)$. At higher concentrations of vacancies, the difference between the two cases (a) and (b) disappears, which agrees with the experimentally observed behavior of Young's modulus in fig. 1.

Fig. 2 shows the thermal conductivity as a function of n_{def} at $T = 300 \text{ K}$. As is seen, the enhancement of k takes place in the range of $2.8 \times 10^{12} \text{ cm}^{-2} \leq n_{def} \leq 5.3 \times 10^{13} \text{ cm}^{-2}$ only. The explanation is as follows: at high temperatures the normal and umklapp scattering mechanisms are of the greatest importance and, in this case, k strongly depends on $v\lambda$ [12]. In turn, $v\lambda$ is a function of E_{2D} in accordance with eq. (1) and, therefore, it depends on n_{def} in this region.

Accordingly, we have obtained the increased k at small concentrations of vacancies up to the value close to $5 \times 10^{13} \text{ cm}^{-2}$ with the maximum gain at $n_{def} \sim 7 \times 10^{12} \text{ cm}^{-2}$ which corresponds to the maximum of Young's modulus.

CONCLUSION

We have found a marked increase in the thermal conductivity of grapheme, which is a direct consequence of the experimentally observed effect of ultrahigh stiffness at low densities of vacancy defects. Our study shows that, in a limited range of defect concentrations, the thermal transport demonstrates a rather unique behavior. Namely, the growing number of defects provokes the enhancement of the thermal conductivity in a wide temperature range. Physically, this follows from the fact that after about 100 K the three-phonon scattering processes become dominant. They depend on the sound velocities which grow with Young's modulus in some restricted region of n_{def} . This provides the enhancement of the thermal conductivity. Below $T \leq 100$ K the main sources of the phonon scattering are sample border and point defects so that a strong increase in graphene stiffness has no effect on the thermal conductivity. Notice that our finding can be of importance in the development of graphene based thermoelectric devices.

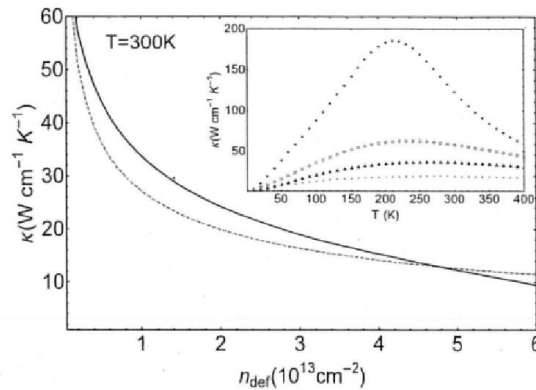


Fig. 2. (Colour online) Thermal conductivity vs. the concentration of vacancies in a $2.9 \mu\text{m}$ wide ribbon for actual (solid line) and constant (dashed line) sound velocities. The insert shows the calculated thermal conductivity vs. temperature with the experimentally observed values of Young's modulus for $n_{def} = 0$ (circles), $2 \times 10^{12} \text{ cm}^{-2}$ (squares), $8 \times 10^{12} \text{ cm}^{-2}$ (triangles), $3 \times 10^{13} \text{ cm}^{-2}$ (stars).

ACKNOWLEDGEMENTS

This work is supported by University Grants Commission, New Delhi (Grant No. PDFSS-2011-12-SC-UTT-2848), India. The authors are thankful to Prof. Jai Shanker, Department of Physics, Institute of Basic Science, Khandari Campus, Agra.

REFERENCES

1. Lopez-Polin, G., Gomez-Navarro, C., Parente, V., Guinea, F., Katsnelson, M.I., Perez-Murano, F. and Gomez-Herrero, J., *Nat. Phys.*, **11**, 26 (2015).
2. Kvashnin, D.G. and Sorokin, P.B., *J. Phys. Chem. Lett.*, **6**, 2384 (2015).
3. Nika, D.L. and Balandin, A.A., *J. Phys. Condens Matter.*, **24**, 33203 (2012).

4. Balandin, A.A., *Nat. Mater.*, **10**, 569 (2011).
5. Nika, D.L., Askerov, A.S. and Balandin, A.A., *Nano Lett.*, **12**, 3238 (2012).
6. Munoz, E., Lu, J. and Yakobson, B.I., *Nano Lett.*, **10**, 1652 (2010).
7. Callaway, J., *Phys. Rev.*, **113**, 1046 (1959).
8. Alofi, A. and Shrivastava, G.P., *Phys. Rev.*, **B 87** 115421 (2013).
9. Slack, G.A. and Galginaitis., *Phys. Rev.*, **A 133**, 253 (1964).
10. Morelli, D.T., Heremans, J.P. and Slack, G.A., *Phys. Rev.*, **B 66**, 195304 (2002).
11. Mounet, N. and Marzart, N., *Phys. Rev.*, **B 71**, 205214 (2005).
12. Nika, D.L., Pokatilov, E.P., Askerov, A.S. and Balandin, A.A., *Phys. Rev.*, **B 79**, 155413 (2009).

